Heterozygous Mutations in *MAP3K7*, Encoding TGF-β-Activated Kinase 1, Cause Cardiospondylocarpofacial Syndrome

Carine Le Goff,[1] Curtis Rogers,[2] Wilfried Le Goff,[3] Graziella Pinto,[4] Damien Bonnet,[5] Maya Chrabieh,[6] Olivier Alibeu,[7] Patrick Nistchke,[8] Arnold Munnich,[1] Capucine Picard,[6,9,10] and Valérie Cormier-Daire[1,*]

Cardiospondylocarpofacial (CSCF) syndrome is characterized by growth retardation, dysmorphic facial features, brachydactyly with carpal-tarsal fusion and extensive posterior cervical vertebral synostosis, cardiac septal defects with valve dysplasia, and deafness with inner ear malformations. Whole-exome sequencing identified heterozygous *MAP3K7* mutations in six distinct CSCF-affected individuals from four families and ranging in age from 5 to 37 years. *MAP3K7* encodes transforming growth factor β (TGF-β)-activated kinase 1 (TAK1), which is involved in the mitogen-activated protein kinase (MAPK)-p38 signaling pathway. MAPK-p38 signaling was markedly altered when expression of non-canonical TGF-β-driven target genes was impaired. These findings support the loss of transcriptional control of the TGF-β-MAPK-p38 pathway in fibroblasts obtained from affected individuals. Surprisingly, although TAK1 is located at the crossroad of inflammation, immunity, and cancer, this study reports *MAP3K7* mutations in a developmental disorder affecting mainly cartilage, bone, and heart.

We previously reported a condition characterized by growth retardation, dysmorphic facial features, brachydactyly with carpal-tarsal fusion and extensive posterior cervical vertebral synostosis, cardiac septal defects with valve dysplasia, and deafness with inner ear malformations in two distinct individuals[1] and proposed the acronym of cardiospondylocarpofacial syndrome (CSCF [MIM:157800]) for it. We collected four additional individuals, including three affected individuals from the same family. CSCF has overlapping but also distinct features from the acromelic dysplasias (MIM: 277600, 102370, 231050, and 139210), which are associated with an impairment of TGF-β signaling. We therefore hypothesized that the molecular basis of CSCF might be related to the TGF-β signaling pathway. Here, we describe dominant mutations of *MAP3K7* [MIM: 602614], encoding TGF-β-activated kinase 1 (TAK1), in six individuals with CSCF.

We collected DNA samples of six individuals from four unrelated families affected by CSCF (Figure 1 Table 1). Written informed consent was obtained from all the individuals, in agreement with the French ethics committee. They all fulfilled the following inclusion criteria: short stature, short hands, carpal-tarsal fusion and vertebral synostosis, facial dysmorphism, and cardiac defects (Table 1). The series included three simplex cases and one case of father to children transmission (family 3, Figure 1). The individuals ranged in age from 5 to 37 years. None of them had severe or recurrent bacterial infections. Three of them (P1, P2, and P3) had normal immunologic workups, including T cell, B cell, and NK immunophenotypes, IgG, IgA, and IgM plasma levels, and positive specific diphtheria and pneumococcus antibodies.

To identify the molecular basis of CSCF, we performed exome sequencing in four CSCF-affected probands, including two simplex and two familial cases (father and son). Enrichment was performed by hybridization of shotgun fragment libraries to Agilent SureSelect in solution capture assays. Using the Solid 3.5 (Life Technologies), we generated and analyzed an average 5.1 Gb of sequence data per sample to achieve more than 40× median coverage of the targeted exome (38 Mb, ~18,000 genes). We focused our analysis on nonsynonymous variants, splice-acceptor and donor-site mutations, and coding insertions or deletions, anticipating that synonymous variants were far less likely to be pathogenic. We regarded variants as previously unidentified if they were absent from control populations and from all datasets, including dbSNP build 129, the 1000 Genomes Project, and in-house exome data (Imagine Institute). Under an autosomal-dominant mode of inheritance, exome analysis identified one candidate gene, *MAP3K7*, which encodes TAK1. Exome analysis detected three distinct heterozygous *MAP3K7* variants

[1]Department of Medical Genetics, Reference Center for Skeletal Dysplasia, INSERM UMR 1163, Laboratory of Molecular and Physiopathological Bases of Osteochondrodysplasia, Paris Descartes-Sorbonne Paris Cité University, AP-HP, Institut Imagine, and Hôpital Universitaire Necker-Enfants Malades, 75015 Paris, France; [2]Greenwood Genetic Center Greenville Office, 14 Edgewood Drive, Greenville, SC 29605, USA; [3]Sorbonne Universités, UPMC Univ. Paris 06, INSERM, ICAN, Institute of Cardiometabolism and Nutrition (UMR_S1166), Integrative Biology of Atherosclerosis Team, 91 Boulevard de l'Hôpital, 75013 Paris, France; [4]Pediatric Endocrinology, Gynecology and Diabetes, Centre des Maladies Endocriniennes Rares de la Croissance, Hôpital Universitaire Necker-Enfants Malades, 75015 Paris, France; [5]Centre de Référence Malformations Cardiaques Congénitales Complexes–M3C, Hôpital Universitaire Necker-Enfants Malades, Université Paris Descartes, 75015 Paris, France; [6]Necker Branch, Laboratory of Human Genetics of Infectious Diseases, UMR 1163, Université Paris Descartes, Sorbonne Paris Cité, Institut Imagine, Hôpital Necker-Enfants Malades, 75015 Paris, France; [7]Genomic Platform, INSERM UMR 1163, Paris Descartes-Sorbonne Paris Cité University, Institut Imagine, 75015 Paris, France; [8]Bioinformatic Platform, INSERM UMR 1163, Paris Descartes-Sorbonne Paris Cité University, Institut Imagine, 75015 Paris, France; [9]Pediatric Hematology-Immunology-Rheumatology Unit, AP-HP, Hôpital Universitaire Necker-Enfants Malades, 75015 Paris, France; [10]Study Center of Immunodeficiencies, Hôpital Universitaire Necker-Enfants Malades, AP-HP, 75015 Paris, France
*Correspondence: valerie.cormier-daire@inserm.fr
http://dx.doi.org/10.1016/j.ajhg.2016.06.005.

Figure 1. Clinical and Radiological Features of CSCF Syndrome
Clinical features in family 3 (father and son). Individual 5 is shown at birth and the age of 5 years (A and B), and individual 3 is shown at the age of 37 years (C–F). Note hypertelorism, downslanting palpebral fissures, ptosis, full cheeks, long philtrum, and short extremities. Radiological features are shown in individual 5 at 5 years of age (G and I) and in individual 6 at age 22 (H and J). Note the hand capitate-hamate synostosis and brachydactyly; note the spine posterior synostosis.

([GenBank: NM_145331.2] UCSC Genome Browser (hg19), transcript B encodes the longest isoform) in the two simplex cases (individuals 2 and 1) and the familial form (individuals 3 and 5, family 3), respectively, namely, c.328G>T (p.Gly110Cys), c.130_135delAGAGGA (p.Arg44_Gly45delin), and c.148_150delGTT (p.Val50del), respectively. These results were confirmed by Sanger sequencing. The 17 coding exons of *MAP3K7* encode a 606-residue protein composed of a serine-threonine/tyrosine-protein kinase catalytic domain (from amino acid [aa] 30 to 306) and a C-terminal coiled-coil domain (aa 533 to 564). Direct sequence analysis of the coding regions in one additional individual with CSCF led to identification of a different heterozygous missense mutation in the kinase domain of TAK1 (c.721T>A, p.Trp241Arg, individual 6). All variants were predicted to be pathogenic via the SIFT MutationTaster and PolyPhen-2 algorithms and occurred at highly conserved amino acids across species. They were absent from 200 ethnicity-matched controls and 5,483 in-house exome data with 11,040 distinct samples and from the Exome Aggregation Consortium (ExAC) browser and were not observed in the parents of the three simplex probands, confirming that they occurred de novo. For the familial case (family 3), the same deletion was identified in the affected daughter (c.148_150delGTT) and was absent in the paternal grandparents, indicating de novo occurrence in the father.

TAK1 is encoded by *MAP3K7* and belongs to the mitogen-activated protein kinase kinase kinase family (MAP3K). This protein is a serine-threonine kinase that is activated by TGF-β.[2,3] Other stimuli can activate TAK1, such as environmental stress, proinflammatory cytokines (interleukin [IL]-1), the tumor necrosis factor alpha (TNF-α), and Toll-like receptor agonists such as lipopolysaccharides (LPSs). TAK1 activation involves its binding to the TAK-associated binding proteins 1–3 (TAB1, TAB2, and TAB3) and its interaction with the E3 ubiquitin ligase tumor necrosis factor receptor-associated factor (TRAF) 6, which directly interacts with a consensus motif present in TGF-βRI.[4,5] TAK1 mediates activation of c-Jun N-terminal kinases and the MAPK-p38 and NF-κB pathways. TAK1 is involved in the regulation of innate and adaptive immunity and is also at the crossroad of various receptors involved in inflammation.[6,7]

In order to determine the functional impact of *MAP3K7* mutations, we assessed the level of TAK1 in cultured skin fibroblasts by western blot analysis. We found comparable amounts of TAK1 in the fibroblasts from affected

Table 1. Clinical Manifestations of Individuals with CSCF

	Family 1	Family 2	Family 3			Family 4
	Individual 1	Individual 2	Individual 3 (Father)	Individual 4 (Daughter)	Individual 5 (Son)	Individual 6
MAP3K7 amino acid change	p.Arg44_Gly45del	p.Gly110Cys	p.Val50del	p.Val50del	p.Val50del	p.Trp241Arg
Epidemiology						
Gender	F	F	M	F	M	F
Ancestry	Morocco, Algeria	France	France	France	France	China, USA
Mother's age at birth (years)	36	40	26	27	32	39
Father's age at birth (years)	37	37	28	27	32	31
Growth						
Birth (weeks of gestation)	40	38	?	38	41	41
Weight, g (SD)	2,070 (< 3)	3,090 (0)	?	3,000 (0)	3,125 (0)	2,860
Length, cm (SD)	51.5 (+0.5)	46.5 (−0.7)	?	47 (−0.5)	47 (−1)	45
OFC, cm (SD)	35.9 (+1)	36.5 (+2.5)	?	35.5 (+1)	35 (0)	?
Last Evaluation						
Age (years)	13	16	37	death D9	5	22
Weight, kg (SD)	25 (−3)	37 (−2.5)	55	–	12 (−2.5)	39
Length, cm (SD)	124 (−5)	145 (−2.5)	165	–	92 (−3.5)	137.9
OFC, cm (SD)	54 (+1)	54 (M)	54	–	50 (M)	53.3
GH Treatment						
Yes or no (start age in years)	+ (5)	+ (10)	–	NA	+ (5)	–
Facial Features						
Strabismus	+	–	+	–	+	–
Hypertelorism	+	+	+	+	+	–
Distopia canthorum	+	+	–	–	–	+
Slant-up palpebral fissures	+	+	+	+	+	–
Peri/supra-orbital fullness	+	+	+	+	+	+
Full cheeks	+	+	+	+	+	+
Posteriorly rotated ears	+	+	+	+	+	–
Anteverted nares	+	+	–	+	+	–
Long philtrum	+	+	+	+	+	–
Skeletal Features						
Delayed bone age	+	+	–	NA	+	–
Joint laxity	+	+	+	NA	+	+
Short extremities	+	+	+	NA	+	+
Brachydactyly	+	+	+	NA	+	+
Cone-shaped epyphysis	+	-	NA	NA	–	NA
Carpal fusion	+	+	NA	NA	+	+
Tarsal fusion	+	+	NA	NA	+	?
Cervical vertebral fusion	+	+	+	NA	+	+

(*Continued on next page*)

Table 1. ***Continued***

	Family 1	Family 2	Family 3			Family 4
	Individual 1	**Individual 2**	**Individual 3 (Father)**	**Individual 4 (Daughter)**	**Individual 5 (Son)**	**Individual 6**
Dorsal spine synostosis	+	–	–	NA	–	–
Dorsal scoliosis	+	–	–	NA	–	mild
Back brace	night	–	–	NA	–	–
Heart						
Septal defect	VSD	ASD	–	–	–	–
Valve dysplasia	multiple valves	multiple valves	mitral valve	tricuspid valve and pulmonary stenosis	prolapsus mital valve	innocent murmur and tachycardia
Digestive System						
Feeding difficulties (birth)	+	+	+	NA	+	+
Severe failure to thrive	+	+	+	NA	+	+
Oro-pharyngeal difficulties	+	+	+	NA	–	–
Gastro-esophageal reflux (Nissen fundoplication)	+	+	+	NA	+	–
Gastrostomy removal (age, years)	+ (3.8)	+ (5.4)	–	NA	–	–
Genitourinary System						
Vesico-ureteral reflux	+	–	–	horseshoe kidney	–	–
Abnormal genitalia	–	–	small testis right ectopia	–	small testis right ectopia	–
Ear, Nose, and Throat						
Recurrent otitis	+	+	+	NA		
Bilateral conductive deafness	+	+	+	NA	+	+
Inner ear malformation	+ (EVA)	+	+	NA	+	ossicle synostoses
Other						
	–	–	benign parotid tumor	diaphragmatic hernia	–	–

+, present; –, not present; VSD, ventricular septal defect; ASD, atrial septal defect; EVA, enlarged vestibular aqueduct; NA, not applicable; OFC, occipital frontal circumference

individuals (1, 2, and 3), as compared to endogenous TAK1 amounts in age- and passage-matched control skin fibroblasts (Figure 2A).

To analyze the activity level of TAK1, we performed western blot analysis with an anti-phospho-TAK1 antibody in order to test its autoactivation. Although phosphorylation levels were variable among affected subjects, our finding of phosphorylated TAK1 in both affected subjects and control individuals supports activation of TAK1 in all cases (Figure 2A).

Under TGF-β stimulation, activated TAK1 normally phosphorylates MKK3 and MKK6, which in turn phosphorylate and activate the p38 family of MAPKs. Considering the importance of the MAPK-p38 signaling in skeletogenesis, we focused on the functional impact of *MAP3K7* mutations on this pathway.[8] We determined the level of phospho-p38 in CSCF fibroblast lysates and observed a decreased level of phospho-p38 in CSCF cell lysates as compared that in controls, although total p38 levels were not affected (Figure 2A).

A fungal resorcylic lactone, 5Z-7-oxozeaenol, is known to inhibit the kinase activity of purified TAK1.[9] This compound has no significant effect on other MAP3K family members. We performed western blot analysis on control fibroblast lysates (same controls in Figures 2A and 2B) to evaluate the level of phospho-p38 activation under this condition. In the presence of this TAK1 inhibitor, the level of phospho-p38 was comparable to that previously observed in the CSCF fibroblasts and in unstimulated cells. (Figure 2B).

Considering the pivotal role of TAK1 in non-canonical TGF-β and bone morphogenetic proteins (BMPs)

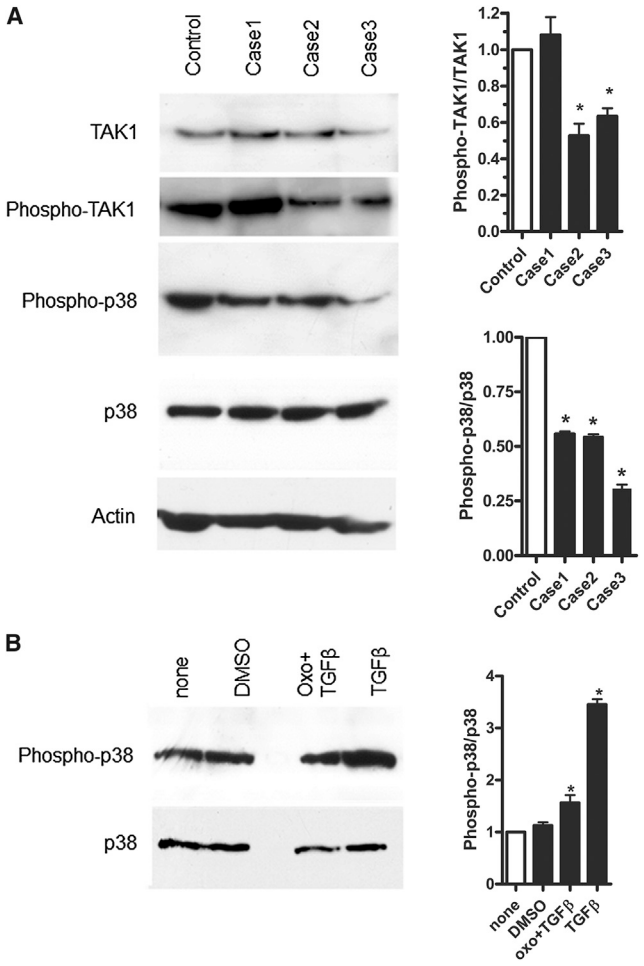

Figure 2. Functional Impact of *MAP3K7* Mutations on CSCF Fibroblasts

(A) Characterization of TAK1, phospho-TAK1, phospho-p38, and p38 protein levels in CSCF primary fibroblast lysates versus those in a control, according to immunoblot, $^*p < 0.05$ ($n = 3$). For western blot analysis of phospho-TAK1, p38, and phospho-p38, cell lysates were obtained from skin fibroblasts (control individual and individuals 1, 2, and 3) after stimulation with TGF-β (10 ng/mL) during 2 hr in serum-free medium. The immunoblot shows a comparable level of TAK1 in the control and affected individual samples. The level of phospho-p38 was altered in response to TGF-β in mutant fibroblasts, in comparison to controls. The levels of phospho-TAK1/TAK1 and phospho-p38/total p38 were quantified with IMAGEJ analysis software. The actin antibody was used to assess loading variation. Anti-actin (Abcam, no. 8226), anti-TAK1 (Abcam, no. 167625), anti-phospho-TAK1 (phospho-Ser412, Cell Signaling, no. 9339), anti-p38 (phospho Y182 + T180, Abcam, no. 27986), and phospho-p38 (Cell Signaling, no. 9216) antibodies, as well as the secondary antibody (goat anti-rabbit, GE Healthcare, no. NA934V), were used.

(B) Inhibition of TAK1 by 5Z-7-oxozeaenol in treated primary fibroblasts versus in a non-treated control (none). Analysis of phospho-p38 versus p38 by western blot, $^*p < 0.05$ ($n = 3$). For 5Z-7-oxozeaenol (500 nM, Sigma) treatment, control fibroblasts were pretreated with 500 nM 5Z-7-oxozeaenol for 30 min and then stimulated with TGF-β (same concentration) in serum-free medium. The material used in this experiment was from the same control as in Figure 2A. The levels of phospho-p38 to total p38 were quantified with IMAGEJ analysis software.

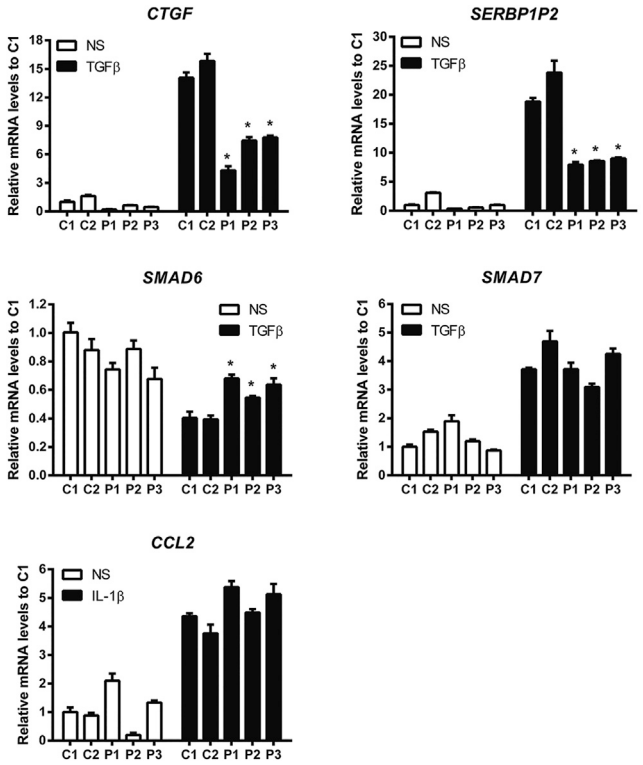

Figure 3. Real-Time qPCR Analysis of TGF-β- or IL-1β-Driven Target Gene Expression

Quantification of CTGF, SERBP1P2 (MAPK-TGF-β signaling pathway) and SMAD6, SMAD7 (inhibitors), or CCL2 mRNA expression after TGF-β or IL-1β stimulation, respectively, in two control (C1 and C2) and three case fibroblasts (P1, P2, and P3). $n = 6$, values are expressed as means ± SE. $^*p < 0.05$ versus C1. White bars represent non-stimulation (NS), black bars represent stimulation with either with TGF-β or IL-1.

pathways, we questioned the ability of these mutants to conduct TGF-β and IL-1β-driven transcription. Expression of mRNA was normalized to housekeeping genes (human heat shock protein 90 kDa alpha [MIM: 140571], human non-POU domain-containing octamer-binding protein [MIM: 300084], and human 18S rRNA [MIM: 611133]). Data were expressed as a fold change in mRNA expression relative to control values. Real- time qPCR analyses showed decreased mRNA expression of downstream TGF-β target genes, namely *CTGF* (connective tissue growth factor [MIM: 121009]) and *SERBP1P2* (plasminogen activator inhibitor 1 [MIM: 173360]) and opposite effects on an inhibitor of MAPK-p38, *SMAD6* (MIM: 602931), with an increased expression compared to controls. The mRNA expression of SMAD7 (MIM: 602932) was unchanged. Similarly, no change on the selected IL-1β target gene (CCL2 [MIM: 158105]) was observed (Figure 3).

Here, we report on identification of heterozygous *MAP3K7* mutations in six individuals clinically diagnosed with CSCF from four unrelated families and provide evidence for an autosomal-dominant mode of inheritance. The cardiac and skeletal malformations, deafness, and facial features characteristic of this syndrome support an

important previously unknown role of TAK1 during development.

All heterozygous mutations were located in the kinase domain of TAK1. Our observation of TAK1 phosphorylation in CSCF fibroblasts does not allow us to conclude on the ability of TAK1 to autoactivate, but strongly suggests that mutant TAK1 does not inhibit autophosphorylation.

Functional TAK1 is a mediator of the MAPK-p38 pathway. Our findings of an impaired stimulation of non-canonical TGF-β-driven target gene expression associated with a decrease of phospho-p38 in response to TGF-β further support a defect in the transcriptional regulation of the MAPK-p38 pathway. Indeed, we observed a downregulation of expression of both *CTGF* and *SERBP1P2*, two genes directly under the control of the MAPK-TGF-β-TAK1-TRAF6 pathway.[3–16]Yet, lack of *SMAD6* repression upon TGF-β stimulation in CSCF demonstrates the maintenance of the negative regulation loop on MAPK-p38 signaling. Indeed, it has been reported that SMAD6, but not SMAD7, negatively regulates TGF-β-induced activation of the p38 MAPK-JNK pathway.[16]

Of note, homozygous *tak1*-deficient mice died early in embryonic development, at day 9.5.[7] Deletion of *tak1* in chondro-osteo progenitor cells led to severe postnatal growth retardation, a key feature of the CSCF syndrome. Conditional knockout of *tak1* in chondrocytes resulted in skeletal defects, including an impairment of both chondrocyte proliferation and maturation.[10] Deletion of *tak1* in mouse limb mesenchyme caused joint fusions and revealed another hitherto unknown role of TAK1 in chondrocyte columns organization and terminal maturation.[10] Altogether, these data support that TAK1 is required to insure the normal organization of chondrocytes in the growth plate. TAK1 also plays a major role in articular cartilage development.[8] Finally, in the mouse model, targeted ablation of tak1 in osteoblasts showed craniofacial defects, supporting that tak1 is also essential for maintaining normal pre- and postnatal bone formation in vivo.[11] This function might also explain the facial features observed in individuals with CSCF.

The identification of heterozygous *MAP3K7* mutations in CSCF expands the *MAP3K7* phenotypic spectrum to developmental disorder. Of note, there are no overlapping features between CSCF and the phenotype of an individual reported with an interstitial 6q deletion encompassing *MAP3K7*.[17] Until now, TAK1 has been considered as either a tumor suppressor or a promoter depending on the context and cell type. Somatic *MAP3K7* mutations have been observed in various human cancers, such as liver and prostate cancer. The deletion of the 6q15 region containing *MAP3K7* is associated with prostate cancer.[12] Disruption of TAK1 in hepatocytes leads to hepatic carcinogenesis.[13] Individuals with B cell lymphoma might have pathogenic variants in *MAP3K7*.[14] In parallel, prevention of cancer development might benefit from TAK1 inhibition—for example, to stop development of lung metastasis of breast cancer. TAK1 has been shown to be essential for lymphoma survival.[15] Interestingly, none of the CSCF-affected individuals developed any cancer. Long-term follow-up will reveal whether or not these mutations are associated with an increased neoplastic risk. Moreover, none of the CSCF-affected individuals exhibited clinical symptoms related to immunodeficiency, although TAK1 is involved in regulation of innate and adaptive immunity.[7]

In conclusion, this study reports on *MAP3K7* mutations in a developmental disorder. Because TAK1 is located at the crossroad of inflammation, immunity, and cancer, long-term follow-up will require continued monitoring of individuals for disimmunity and cancer development. Ongoing studies will hopefully contribute to further elucidation of the context-dependent mechanisms of TAK1 disruption and might promote development of pharmacological strategies.

Supplemental Data

Supplemental Data include one table and can be found with this article online at http://dx.doi.org/10.1016/j.ajhg.2016.06.005.

Acknowledgments

We are grateful to the affected subjects and their families. We would like to thank J.L. Casanova for his comments. This research program has received a state subsidy managed by the National Research Agency under the Investments for the Future program bearing the reference ANR-10-IAHU-01.

Received: March 8, 2016
Accepted: June 1, 2016
Published: July 14, 2016

Web Resources

1000 Genomes, http://www.1000genomes.org
OMIM, http://www.omim.org/
ExAC Browser, http://exac.broadinstitute.org/
GenBank, http://www.ncbi.nlm.nih.gov/genbank/
PolyPhen-2, http://genetics.bwh.harvard.edu/pph2/
SIFT, sift.jcvi.org
UCSC Genome Browser, http://genome.ucsc.edu

References

1. Sousa, S.B., Baujat, G., Abadie, V., Bonnet, D., Sidi, D., Munnich, A., Krakow, D., and Cormier-Daire, V. (2010). Postnatal growth retardation, facial dysmorphism, spondylocarpal synostosis, cardiac defect, and inner ear malformation (cardiospondylocarpofacial syndrome?)–a distinct syndrome? Am. J. Med. Genet. A. *152A*, 539–546.
2. Yamaguchi, K., Shirakabe, K., Shibuya, H., Irie, K., Oishi, I., Ueno, N., Taniguchi, T., Nishida, E., and Matsumoto, K. (1995). Identification of a member of the MAPKKK family as a potential mediator of TGF-beta signal transduction. Science *270*, 2008–2011.
3. Takaesu, G., Kishida, S., Hiyama, A., Yamaguchi, K., Shibuya, H., Irie, K., Ninomiya-Tsuji, J., and Matsumoto, K. (2000).

TAB2, a novel adaptor protein, mediates activation of TAK1 MAPKKK by linking TAK1 to TRAF6 in the IL-1 signal transduction pathway. Mol. Cell *5*, 649–658.

4. Scholz, R., Sidler, C.L., Thali, R.F., Winssinger, N., Cheung, P.C., and Neumann, D. (2010). Autoactivation of transforming growth factor beta-activated kinase 1 is a sequential bimolecular process. J. Biol. Chem. *285*, 25753–25766.
5. Delaney, J.R., and Mlodzik, M. (2006). TGF-beta activated kinase-1: new insights into the diverse roles of TAK1 in development and immunity. Cell Cycle *5*, 2852–2855.
6. Sato, S., Sanjo, H., Takeda, K., Ninomiya-Tsuji, J., Yamamoto, M., Kawai, T., Matsumoto, K., Takeuchi, O., and Akira, S. (2005). Essential function for the kinase TAK1 in innate and adaptive immune responses. Nat. Immunol. *6*, 1087–1095.
7. Gunnell, L.M., Jonason, J.H., Loiselle, A.E., Kohn, A., Schwarz, E.M., Hilton, M.J., and O'Keefe, R.J. (2010). TAK1 regulates cartilage and joint development via the MAPK and BMP signaling pathways. J. Bone Miner. Res. *25*, 1784–1797.
8. Greenblatt, M.B., Shim, J.H., Zou, W., Sitara, D., Schweitzer, M., Hu, D., Lotinun, S., Sano, Y., Baron, R., Park, J.M., et al. (2010). The p38 MAPK pathway is essential for skeletogenesis and bone homeostasis in mice. J. Clin. Invest. *120*, 2457–2473.
9. Ninomiya-Tsuji, J., Kajino, T., Ono, K., Ohtomo, T., Matsumoto, M., Shiina, M., Mihara, M., Tsuchiya, M., and Matsumoto, K. (2003). A resorcylic acid lactone, 5Z-7-oxozeaenol, prevents inflammation by inhibiting the catalytic activity of TAK1 MAPK kinase kinase. J. Biol. Chem. *278*, 18485–18490.
10. Gao, L., Sheu, T.J., Dong, Y., Hoak, D.M., Zuscik, M.J., Schwarz, E.M., Hilton, M.J., O'Keefe, R.J., and Jonason, J.H. (2013). TAK1 regulates SOX9 expression in chondrocytes and is essential for postnatal development of the growth plate and articular cartilages. J. Cell Sci. *126*, 5704–5713.
11. Liu, W., Chang, B.L., Cramer, S., Koty, P.P., Li, T., Sun, J., Turner, A.R., Von Kap-Herr, C., Bobby, P., Rao, J., et al. (2007). Deletion of a small consensus region at 6q15, including the MAP3K7 gene, is significantly associated with high-grade prostate cancers. Clin. Cancer Res. *13*, 5028–5033.
12. Inokuchi, S., Aoyama, T., Miura, K., Osterreicher, C.H., Kodama, Y., Miyai, K., Akira, S., Brenner, D.A., and Seki, E. (2010). Disruption of TAK1 in hepatocytes causes hepatic injury, inflammation, fibrosis, and carcinogenesis. Proc. Natl. Acad. Sci. USA *107*, 844–849.
13. Compagno, M., Lim, W.K., Grunn, A., Nandula, S.V., Brahmachary, M., Shen, Q., Bertoni, F., Ponzoni, M., Scandurra, M., Califano, A., et al. (2009). Mutations of multiple genes cause deregulation of NF-kappaB in diffuse large B-cell lymphoma. Nature *459*, 717–721.
14. Buglio, D., Palakurthi, S., Byth, K., Vega, F., Toader, D., Saeh, J., Neelapu, S.S., and Younes, A. (2012). Essential role of TAK1 in regulating mantle cell lymphoma survival. Blood *120*, 347–355.
15. Gu, J., Liu, X., Wang, Q.X., Tan, H.W., Guo, M., Jiang, W.F., and Zhou, L. (2012). Angiotensin II increases CTGF expression via MAPKs/TGF-β1/TRAF6 pathway in atrial fibroblasts. Exp. Cell Res. *318*, 2105–2115.
16. Jung, S.M., Lee, J.H., Park, J., Oh, Y.S., Lee, S.K., Park, J.S., Lee, Y.S., Kim, J.H., Lee, J.Y., Bae, Y.S., et al. (2013). Smad6 inhibits non-canonical TGF-β1 signalling by recruiting the deubiquitinase A20 to TRAF6. Nat. Commun. *4*, 2562.
17. Klein, O.D., Cotter, P.D., Moore, M.W., Zanko, A., Gilats, M., Epstein, C.J., Conte, F., and Rauen, K.A. (2007). Interstitial deletions of chromosome 6q: genotype-phenotype correlation utilizing array CGH. Clin. Genet. *71*, 260–266.

The American Journal of Human Genetics, Volume *99*

Supplemental Data

Heterozygous Mutations in *MAP3K7*, Encoding TGF-β-Activated Kinase 1, Cause Cardiospondylocarpofacial Syndrome

Carine Le Goff, Curtis Rogers, Wilfried Le Goff, Graziella Pinto, Damien Bonnet, Maya Chrabieh, Olivier Alibeu, Patrick Nistchke, Arnold Munnich, Capucine Picard, and Valérie Cormier-Daire

	Coverage	Reads depth (15x)	Reads depth (30x)	Total relevant variants	Variant under dominant model	After in house data analysis	Variant under recessive model	After in house data analysis
Case 1	42	57,8	46	926	27 (clinically associated 16)	1	120 (clinically associated 68)	0
Case 2	40	64	50	972				
Case 3	80	69	60	1385				
Case 5	79	68	59	1064				

Supplemental table 1 WES data